

Non-Gaussian models for critical fluctuations

J. A. Tuszyński, M. J. Clouter, and H. Kiefte

Department of Physics, Memorial University of Newfoundland, St. John's, Newfoundland, Canada A1B 3X7

(Received 18 October 1985)

This paper investigates the role of statistical fluctuations about the equilibrium value of the order parameter in the vicinity of a phase-transition temperature. The systems under consideration are assumed to be of finite size, but the behavior in the thermodynamic limit is also described. Our objective is to examine the simplest exactly solvable model of non-Gaussian static fluctuations for samples of finite size. To this end a Landau form is employed for the model Hamiltonian and various expansions are analyzed in order to describe first- and second-order phase transitions, field-induced transitions, and liquid-vapor critical phenomena. The approach differs from previous treatments primarily in the application of a quartic non-Gaussian model for statistical fluctuations which redresses some of the shortcomings of the standard Gaussian approximation. In particular, it is found that for finite values of V (volume) no singularities exist even at the critical temperature. The treatment is generalized by examining a class of non-Gaussian distribution functions, and particular emphasis is placed on strict adherence to the uniform convergence criterion so that general conclusions can be drawn.

I. INTRODUCTION

As is well known,¹ the approach to criticality is associated with a rapid growth of spatial fluctuations in the order parameter. It has been emphasized^{2,3} that because of the prominent role of fluctuations, the often used Gaussian approximation inevitably fails in the vicinity of the critical temperature. This paper is intended as a study of the feasibility of improving upon the standard Gaussian approximation. The various mathematical models adopted here are of a non-Gaussian form and are formulated so as to satisfy the uniform convergence criterion for the resultant partition function. The results for one particular case which permits exact solutions, namely, the quartic non-Gaussian distribution, have recently been published.⁴ In this paper a class of non-Gaussian models is introduced as a logical generalization of the Gaussian approximation and emphasis is placed on the rigor of the mathematical procedures. These models are applied within the mean-field framework of the Landau theory. The system is initially assumed to be of finite size ($V < \infty$) but a behavior in the thermodynamic limit ($V \rightarrow \infty$) is also discussed. Hamiltonians relevant to first- and second-order phase transitions, both temperature- and field-induced are investigated. The special case of liquid-vapor transitions provides a background for making contact with recent experimental results^{5,6} for molecular nitrogen.

II. STATISTICAL FLUCTUATIONS

It is a well-known precept of statistical mechanics,⁷ that while the measured values of bulk quantities which describe a macroscopic system in equilibrium are always very close to their thermal averages, fluctuations about these average values nevertheless do occur in all situations. For example, in the canonical ensemble the average fluctuation in the energy of an equilibrium system can be calculated as⁸

$$\langle (E - \bar{E})^2 \rangle = \frac{\partial}{\partial \beta} \left[Z^{-1} \frac{\partial Z}{\partial \beta} \right], \quad (1)$$

where the mean energy is $\bar{E} = -Z^{-1}(\partial Z / \partial \beta)$, the partition function is $Z \equiv \text{Tr} \exp(-\beta H)$, H is the Hamiltonian of the system, $\beta \equiv (k_B T)^{-1}$, and k_B is the Boltzmann constant. Given the definition of the heat capacity at constant volume V , $C_V \equiv (\partial \bar{E} / \partial T)_V$, it can be easily shown^{7,8} that the average energy fluctuation is proportional to C_V , i.e.,

$$\langle (E - \bar{E})^2 \rangle = \beta^{-2} C_V, \quad (2)$$

which essentially is the content of the fluctuation-dissipation theorem. Similarly, in the grand canonical ensemble, the average fluctuation in the number of particles \bar{N} is expressed by another form of the fluctuation-dissipation theorem, namely,

$$\langle (N - \bar{N})^2 \rangle = v^{-1} \bar{N}^2 \kappa_T, \quad (3)$$

where $v \equiv \beta V$, $\kappa_T \equiv -(1/V)(\partial V / \partial P)_T$ is the isothermal compressibility, and P is the pressure.

Assuming in general that the macroscopic state of the system can be determined by a set of $(n+1)$ extensive thermodynamic variables x_i ($0 \leq i \leq n$) whose intensive variable counterparts are $X_i \equiv -(\partial E / \partial x_i)$, then statistical fluctuations can be denoted by $\Delta x_i \equiv x_i - \bar{x}_i$. This naturally leads to the consideration of a probability distribution function for these fluctuations known as the Boltzmann distribution, which is a consequence of the principle of equal probability.⁸ Therefore, the probability of creating a fluctuation is given by

$$P(\Delta x_i) = A \exp(-\beta \Delta W), \quad (4)$$

where A is a normalization constant and ΔW denotes the work done in the process. We now adopt the notation $x_0 = -S$, $X_0 = T$ and expand the energy fluctuation ΔE in a Taylor series. Truncation of this series at the second-

order terms yields the first approximation for the probability distribution, i.e.,

$$P(\Delta x_i) = \left[\frac{\det(\chi_{ij}^{-1})}{(2\pi)^n} \right]^{1/2} \exp \left[-\frac{\beta}{2} \sum_{i,j} \chi_{ij}^{-1} \Delta x_i \Delta x_j \right], \quad (5)$$

which is of a Gaussian form. Here, the generalized susceptibility is defined as $\chi_{ij} \equiv \partial x_i / \partial X_j$; χ_{ij}^{-1} is its inverse. As a result, the average fluctuations are once again found to satisfy the fluctuation-dissipation theorem

$$\langle \Delta x_i \Delta x_j \rangle = \chi_{ij}. \quad (6)$$

It should be emphasized that the validity of the Gaussian approximation is quite limited. Whereas in general the approximation is known to work very well in the noncritical region, its results are quite unsatisfactory close to the transition point. A brief discussion of these inadequacies is presented in the next section.

III. THE GAUSSIAN APPROXIMATION

The Gaussian probability distribution function is commonly applied throughout the field of statistical physics and is usually written as

$$P(x) = (2\pi\gamma)^{-1/2} \exp[-(x - \bar{x})^2 / 2\gamma]. \quad (7)$$

It expresses the condition that the statistical variable x is permitted to assume values which are symmetrically distributed about a most probable value \bar{x} , which in this (Gaussian) case coincides with the mean value \bar{x} ,

$$\bar{x} \equiv \int_{-\infty}^{+\infty} x P(x) dx = \bar{x}. \quad (8)$$

The extent to which deviations from \bar{x} , i.e., statistical fluctuations, exist in the system is indicated by the magnitude of the width parameter γ (see Appendix A),

$$\gamma = \int_{-\infty}^{+\infty} (x - \bar{x})^2 P(x) dx. \quad (9)$$

Because of the increasing role of fluctuations in the approach to criticality^{3,4} the Gaussian approximation leads to serious difficulties in describing the critical phenomena. It is apparent, for example, that the large spatial extent of fluctuations is instrumental in driving the system into cooperative behavior which, in turn, signifies the onset of order.⁹ The ordered state can be regarded as an irreversible fluctuation which cannot be accommodated by the Gaussian approximation. The Gaussian approximation is also associated with the unphysical divergence of some important quantities at criticality. This fact is illustrated by the following brief excursion into the mean-field theory.

In the mean-field approach to phase transitions the effective Hamiltonian of the system is assumed to be a function of the equilibrium value of the order parameter $\bar{\sigma}$. Statistical fluctuations about $\bar{\sigma}$ are then calculated by expanding the Hamiltonian in a Taylor series around $\bar{\sigma}$ (Ref. 1) which, in this (Gaussian) case, is truncated at the quadratic term

$$H(\sigma) \cong H_{\text{LG}}(\bar{\sigma}) + Va_2(\sigma - \bar{\sigma})^2 + \dots, \quad (10)$$

where $H_{\text{LG}} = \int d^D r \mathcal{H}_{\text{LG}}$ is the Landau-Ginzburg Hamiltonian whose density is

$$\mathcal{H}_{\text{LG}} = \sum_{k=2}^N A_k \sigma^k + \sum_{k=1}^M B_{2k} (\nabla \sigma)^{2k}, \quad (11)$$

where $A_2 = a\tau$, $\tau \equiv T - T_0$ and D is the dimensionality of the physical space, i.e., $V = L^D$. For second-order phase transitions we only need $N=4$ and $A_3=0$ when $\sigma \rightarrow -\sigma$ under the time reversal. Consequently, we find that⁴ $a_2 = A_2 + 6A_4 \bar{\sigma}^2$ and $\bar{\sigma} = \pm(-a\tau/2A_4)^{1/2}$ when $\tau < 0$ and $\bar{\sigma} = 0$ when $\tau > 0$. The probability distribution function in this case has the obvious Gaussian form (see. Fig. 1)

$$P^v(\sigma) = (Z^v)^{-1} \exp\{-v[\mathcal{H}_{\text{LG}}(\bar{\sigma}) + a_2(\sigma - \bar{\sigma})^2]\}, \quad (12)$$

where the corresponding partition function is given by

$$Z^v = (\pi/va_2)^{1/2} \exp[-v\mathcal{H}_{\text{LG}}(\bar{\sigma})]. \quad (13)$$

These two results are characterized by an unphysical divergence at $\tau=0$ for all values of v . This contradicts the Yang-Lee Theorem¹⁰ which states that for finite-sized systems, the partition function must be finite, since it is a finite sum of finite terms. The same type of divergence exists for all even moments of the probability distribution function

$$\begin{aligned} M_n^v &\equiv (Z^v)^{-1} \int_{-\infty}^{+\infty} (\sigma - \bar{\sigma})^n P^v(\sigma) d\sigma \\ &= [\pi(va_2)^n]^{-1/2} \Gamma\left[\frac{n+1}{2}\right]. \end{aligned} \quad (14)$$

In particular, the second moment which is proportional to the generalized susceptibility is found to be

$$\chi^v \equiv v \langle (\sigma - \bar{\sigma})^2 \rangle = (2a_2)^{-1}. \quad (15)$$

Hence, χ^v diverges at T_c for all values of v and, in fact, it is size independent. Both of these properties are unphysical.

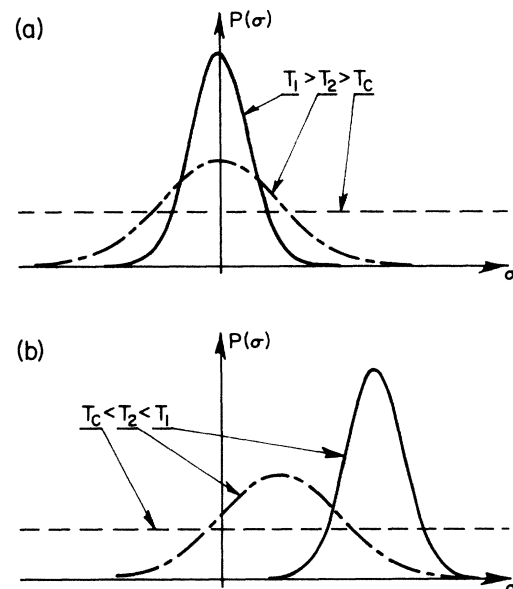


FIG. 1. Supercritical (a) and subcritical (b) behavior of the Gaussian distribution function.

The Gaussian approximation has also been associated with other deficiencies, such as the prediction of incorrect critical exponents.¹ It can, of course, be argued that these difficulties should be attributed to the inadequacies of the Landau model. This is indeed the case with most of the critical exponents since all except α and α' coincide in the two approximations. However, as has been demonstrated in this section, the Gaussian approximation ignores the size dependence at criticality. This is well demonstrated in the particular case of the critical opalescence phenomenon. Experiments indicate¹¹ a mean fluctuation $\langle(\sigma - \bar{\sigma})^2\rangle \sim N^{-1/2}$, while the Landau theory with the superimposed Gaussian approximation leads to⁴ $\langle(\sigma - \bar{\sigma})^2\rangle \sim N^{-1}$. In light of recent interest in finite-size scaling at criticality¹² it is appropriate to undertake an investigation into non-Gaussian models for critical fluctuations.

We conclude here that the Gaussian approximation occurs within the Landau theory as an unnecessary approximation which in itself could constitute a significant restriction upon the applicability of the theory. Any improvement in, or generalization of, the distribution function is clearly less restrictive and will lead to either of two results. First, the predictions of the model may not differ significantly from those obtained under the Gaussian approximation, in which case it may be suitably concluded that the restrictions inherent in the Landau model take precedence. Second, if the predictions are significantly different, it is apparent that the limitations of the Landau model are secondary and that an improved phenomenological description has been achieved. The latter is definitely true in the present treatment because of the qualitative differences between the two models for finite V . The non-Gaussian models eliminate some unphysical divergencies while converging to the Gaussian result at the thermodynamic limit. It is, therefore, apparent that the Landau mean-field approach is capable of further valuable contributions.

IV. PROPERTIES OF NON-GAUSSIAN DISTRIBUTIONS

Consider first a non-Gaussian probability distribution given by (see Fig. 2)

$$P(x) = Z^{-1} \exp[-\lambda_2(x - \bar{x})^2 - \lambda_4(x - \bar{x})^4]. \quad (16)$$

The usual technique applied in such cases¹³ would be to expand $P(x)$ in a series about the Gaussian factor, i.e.,

$$P(x) = Z^{-1} \exp[-\lambda_2(x - \bar{x})^2] \sum_{k=0}^{\infty} \frac{[-\lambda_4(x - \bar{x})^4]^k}{k!}. \quad (17)$$

Provided $\lambda_2 > 0$, the associated partition function can be calculated as (see Appendix B)

$$Z = (\lambda_2)^{-1/2} \sum_{k=0}^{\infty} \left[-\frac{\lambda_4}{\lambda_2^2} \right]^k \frac{\Gamma(2k + \frac{1}{2})}{\Gamma(k)}, \quad (18)$$

and the n th moment as

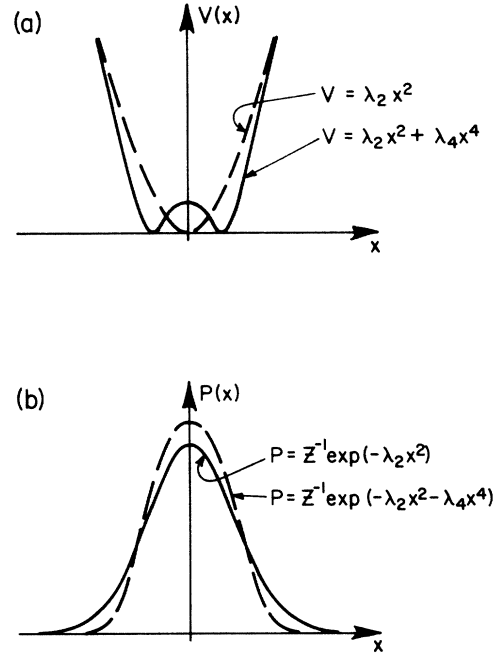


FIG. 2. Schematic representation of the exact and approximate interaction potentials (a) and the corresponding probability distribution functions (b).

$$M_n = Z^{-1} (\lambda_2)^{-(n+1)/2} \sum_{k=0}^{\infty} \left[-\frac{\lambda_4}{\lambda_2^2} \right]^k \frac{\Gamma(2k + (n+1)/2)}{\Gamma(k)}. \quad (19)$$

It has been demonstrated in Appendix B that except for the special case when $\lambda_4/\lambda_2^2 = 0$, which means that $\lambda_4 = 0$ (i.e., the Gaussian approximation) or $\lambda_2 \rightarrow \infty$ [i.e., $P(x) = 0$], both Z and M_n are divergent when expressed by the series of Eqs. (18) and (19), respectively. As is shown later in this section, the expansion of $P(x)$ given in Eq. (17) also violates the uniform convergence criterion.

Provided $\lambda_4 > 0$, an alternative approach to that of Eq. (17) is to expand $P(x)$ about the quartic exponential factor according to

$$P(x) = Z^{-1} \exp[-\lambda_4(x - \bar{x})^4] \sum_{k=0}^{\infty} \frac{[-\lambda_2(x - \bar{x})^2]^k}{k!}. \quad (20)$$

Then, as shown in Appendix C, the associated partition function can be calculated as

$$Z = \frac{1}{2} (\lambda_4)^{-1/4} \sum_{k=0}^{\infty} \left[-\frac{\lambda_2}{(\lambda_4)^{1/2}} \right]^k \frac{\Gamma(k/2 + \frac{1}{4})}{\Gamma(k)} \quad (21)$$

and the n th moment as

$$M_n = Z^{-1} \left(\frac{1}{2} \right) (\lambda_4)^{-(n+1)/4} \times \sum_{k=0}^{\infty} \left[-\frac{\lambda_2}{(\lambda_4)^{1/2}} \right]^k \frac{\Gamma(k/2 + (n+1)/4)}{\Gamma(k)}. \quad (22)$$

This time, however, both Z and M_n are expressed by convergent series, unless $\lambda_4=0$ or $\lambda_2 \rightarrow \infty$.

The result is, therefore, that the first type of expansions is convergent for radius $R \equiv (\lambda_4/\lambda_2^2)=0$ and the second for $R \neq 0$. Hence, they are legitimate in mutually excluded ranges of R .

Furthermore, using a recently published integral,¹⁴ we can provide the following analytical expressions for Z and M_n (see Appendix D) which combine the previous series expansions

$$Z = (2\lambda_4)^{-1/4} \Gamma(\frac{1}{2}) \exp\left\{\frac{\lambda_2^2}{8\lambda_4}\right\} D_{-1/2}[\lambda_2/(2\lambda_4)^{1/2}] \quad (23)$$

and

$$M_n = (2\lambda_4)^{-n/4} \frac{\Gamma((n+1)/2)}{\Gamma(\frac{1}{2})} \frac{D_{-(n+1)/2}[\lambda_2/(2\lambda_4)^{1/2}]}{D_{-1/2}[\lambda_2/(2\lambda_4)^{1/2}]}, \quad (24)$$

where $D_{-\nu}$ is the parabolic cylinder function.¹⁵

Finally, we make some comments on the uniform convergence criterion. It is known from calculus¹⁶ that if $f(x) = \sum_k^\infty f_k(x)$, then $\int_a^b f(x)dx = \sum_k^\infty \int_a^b f_k(x)dx$ if and only if the series $\sum_k^\infty f_k(x)$ is uniformly convergent to $f(x)$ in the entire domain of integration $\langle a, b \rangle$. This means that the sequence of partial sums $[S_m = \sum_k^m f_k(x), m=0, 1, \dots, \infty]$ must uniformly converge to $f(x)$. In our case, $f(x) = x^n \exp(-\lambda_2 x^2 - \lambda_4 x^4)$ and $\langle a, b \rangle = (-\infty, +\infty)$. The two series expansions used here can be written as

$$S'_m = \sum_k^m (-\lambda_2 x^2)^k x^n \exp(-\lambda_4 x^4) / k!$$

and

$$S''_m = \sum_k^m (-\lambda_4 x^4)^k x^n \exp(-\lambda_2 x^2) / k!$$

Since the limits of integration extend to infinity, it is quite obvious that unless $\lambda_4=0$ or $\lambda_2 \rightarrow \infty$, uniform convergence of S''_m to $f(x)$ will not be realized in view of the fact that no power function can match the asymptotic behavior of the exponential function. If, however, $\lambda_4=0$ or $\lambda_2 \rightarrow \infty$, then of course the same conclusion applies to S'_m .

In fact this statement can be generalized to the entire class of probability distribution functions given by

$$P(x) = Z^{-1} \exp(-\lambda_p x^p - \lambda_q x^q). \quad (25)$$

That is, assuming that $q > p$, unless $\lambda_q=0$ or $\lambda_p \rightarrow \infty$, the only correct series expansion of $P(x)$ retains $\lambda_q x^q$ in the exponential. This, together with formulas for Z and M_n is shown in Appendix E. Moreover, for distributions of the type

$$P(x) = Z^{-1} \exp\left[-\sum_{k=m}^M \lambda_k (x - \bar{x})^k\right],$$

the uniform convergence criterion requires the term with

the highest power, i.e., $\lambda_M(x - \bar{x})^M$, to be retained in the exponential while all the other terms can be expanded out, provided $\lambda_M \neq 0$ or $\lambda_m \rightarrow \infty$. In the opposite case, the term with the lowest power, i.e., $\lambda_m(x - \bar{x})^m$, is to be retained in the exponential while all the other terms are being expanded.

In this context it should be noted that the reason why the Gaussian approximation works so well in the noncritical region appears to be that for all practical purposes $\lambda_2^2 \gg \lambda_4$ there. The formulas and criteria arrived at in this section will be applied in the critical region to the various expansions of the Landau Hamiltonian.

V. APPLICATIONS TO THE LANDAU THEORY

A. Second-order phase transitions

In order to improve the probability distribution function $P^v(\sigma)$ of Eq. (12) in the context of second-order phase transitions, we extend the expansion of Eq. (10) as

$$\mathcal{H}(\sigma) \cong \mathcal{H}_{\text{LG}}(\bar{\sigma}) + a_2(\sigma - \bar{\sigma})^2 + a_4(\sigma - \bar{\sigma})^4 + \dots, \quad (26)$$

where, as before, $a_2 = A_2 + 6A_4\bar{\sigma}^2$, $a_4 = A_4$ and both of these coefficients are plotted against temperature in Fig. 3. This expansion can be used to calculate the partition function according to Eq. (23) as

$$Z^v = \Gamma(\frac{1}{2})(2va_4)^{-1/4} \exp\left[-v\mathcal{H}_{\text{LG}}(\bar{\sigma}) + \frac{x^2}{4}\right] D_{-1/2}(x), \quad (27)$$

where $x = (va_2^2/2a_4)^{1/2}$. Similarly, the n th moment of $P^v(\sigma)$ is found from Eq. (24) as

$$M_n^v = (2va_4)^{-n/4} \frac{\Gamma((n+1)/2) D_{-(n+1)/2}(x)}{\Gamma(\frac{1}{2}) D_{-1/2}(x)} \quad (28)$$

and, in particular, the susceptibility function is

$$\chi^v = (8a_4/v)^{-1/2} \frac{D_{-3/2}(x)}{D_{-1/2}(x)}. \quad (29)$$

It is of crucial importance that neither Z^v nor M_n^v diverge at any temperature as long as $V < \infty$. This is in clear contrast to the result obtained using the Gaussian approximation. Here, in fact, these quantities approach finite

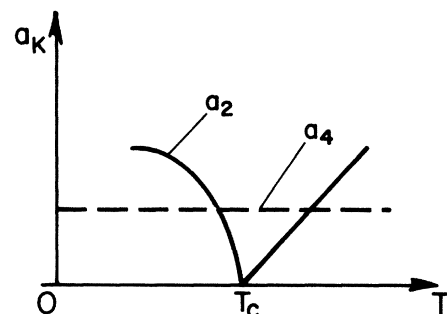


FIG. 3. Schematic plots of the expansion coefficients a_2 and a_4 for second-order phase transitions.

maxima at T_c and these values are found by expanding¹⁵ the D functions in the asymptotic limit of $x \rightarrow 0$ (which means that $T \rightarrow T_c$, while $V < \infty$), i.e.,

$$D_{-a-1/2}(\pm x) \sim \frac{\sqrt{\pi}}{2^{a/2+1/4}\Gamma(\frac{3}{4}+a/2)} \exp[\mp\sqrt{a}x + O(x)]$$

as $|x| \ll 1$. (30)

The resultant maxima are

$$Z_{\max}^v = \pi \exp[-v\mathcal{H}_{\text{LG}}(\bar{\sigma})](4va_4)^{-1/4}/\Gamma(\frac{3}{4}), \quad (31)$$

$$M_{n,\max}^v = (8va_4)^{-n/4} \frac{\Gamma(\frac{3}{4})\Gamma((n+1)/2)}{\Gamma(\frac{1}{2})\Gamma(n/2+\frac{3}{4})}, \quad (32)$$

and

$$\chi_{\max}^v = \frac{2}{3}(v/8a_4)^{1/2}. \quad (33)$$

From Eq. (30) it is obvious that the approach to these maxima is along an exponential curve. The value of the susceptibility maximum increases with volume in proportionality to $V^{1/2}$. Moreover, because of the form of a_2 and x , it is apparent that there is no discontinuity at T_c . The approach to the maxima is faster in the low-temperature (ordered) phase than in the high-temperature (disordered) phase.

Letting $x \rightarrow \infty$ and applying the other asymptotic expansion¹⁵ for $D_{-a-1/2}(x)$, we obtain

$$D_{-a-1/2}(x) \sim \exp\left[-\frac{x^2}{4}\right] x^{-a-1/2}[1+O(1/x)]$$

as $x \rightarrow \infty$. (34)

The following two situations can be investigated: (i) $V < \infty$ and $|\tau| \gg 0$, i.e., finite-size, noncritical systems, or (ii) $V \rightarrow \infty$ and $\tau \neq 0$, i.e., the thermodynamic limit. Note that in the thermodynamic limit the volume expansion precedes the transition to criticality.

It is readily found from Eq. (34) that under these conditions ($x \rightarrow \infty$) the quantities in question, i.e., Z^v , M_n^v , and χ^v , approach their Gaussian estimates which are given in Eqs. (13)–(15). Figure 4(a) illustrates the gradual steepening of the n th moment M_n as x changes from a finite value (solid curve) to infinity (dashed curve). Note the convergence of the two curves for large values of τ . Figure 4(b) is a close-up for χ^v with an exponential fit close to $x=0$. From Eq. (13) with the definition of x the free energy per unit volume is calculated as

$$f = \lim_{V \rightarrow \infty} \left[-\frac{1}{v} \ln Z^v \right]$$

$$= \lim_{v \rightarrow \infty} \left[\frac{1}{2} \left[\frac{\ln a_2}{v} + \frac{\ln v}{v} \right] - \frac{\ln \Gamma(\frac{1}{2})}{v} + \mathcal{H}_{\text{LG}}(\bar{\sigma}) \right]$$

$$= \mathcal{H}_{\text{LG}}(\bar{\sigma}), \quad (35)$$

which leads to the classical critical exponents obtained in the thermodynamic limit.

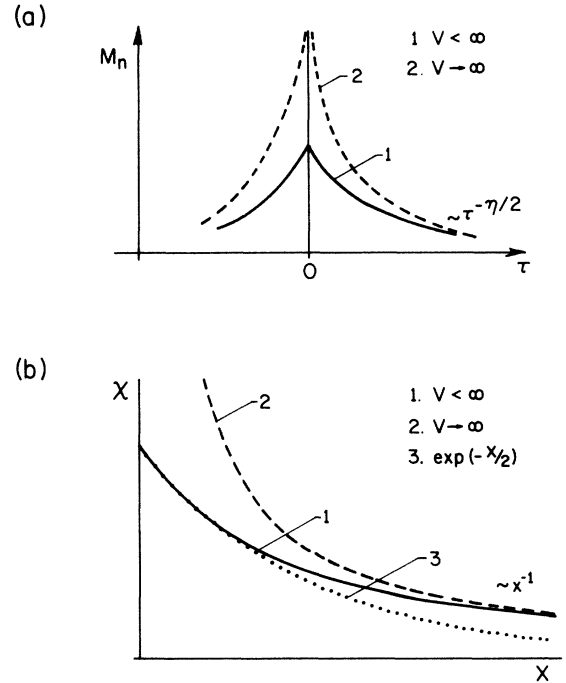


FIG. 4. (a) The gradual steepening of the n th moment M_n of the quartic Gaussian distribution function as the volume of the sample tends to infinity. (b) The plot of χ^v for $V < \infty$ (solid curve), $V \rightarrow \infty$ (dashed curve), and an exponential fit (dotted curve).

B. First-order phase transitions

In order to properly describe the first-order phase transitions, the Landau-Ginzburg Hamiltonian must be taken with $N=6$ and $A_4 < 0$. Then, the series expansion of $\mathcal{H}(\sigma)$ around $\bar{\sigma}$ is

$$\mathcal{H}(\sigma) \cong \mathcal{H}_{\text{LG}}(\bar{\sigma}) + a_2(\sigma - \bar{\sigma})^2 + a_4(\sigma - \bar{\sigma})^4 + a_6(\sigma - \bar{\sigma})^6 + \dots, \quad (36)$$

where

$$\mathcal{H}_{\text{LG}}(\bar{\sigma}) = A_2\bar{\sigma}^2 + A_4\bar{\sigma}^4 + A_6\bar{\sigma}^6,$$

$$a_2 = A_2 + 6A_4\bar{\sigma}^2 + 15A_6\bar{\sigma}^4 \geq 0,$$

$$a_4 = A_4 + 15A_6\bar{\sigma}^2,$$

and

$$a_6 = A_6.$$

The value of $\bar{\sigma}$ is found by minimizing \mathcal{H}_{LG} as

$$\bar{\sigma} = \pm \{ [-A_4 - (A_4^2 - 3aA_6\tau)^{1/2}] / 3A_6 \}^{1/2} \quad (37)$$

for $T \leq T_c^*$ and $\bar{\sigma} = 0$ for $T > T_c^*$. The transition temperature is $T_c^* = T_c + A_4^2/4aA_6$. A couple of points should be emphasized in this connection. First, the range of stability of the equilibrium phases overlaps since the ordered phase is stable for $T \leq T_0 \equiv T_c + A_4^2/3aA_6$ and the disordered phase is stable for $T \geq T_c$. Hence, there exist ranges of metastability for the two phases which coexist between T_c and T_0 . This is illustrated in Fig. 5. Second, depending on the type of the sample there can be

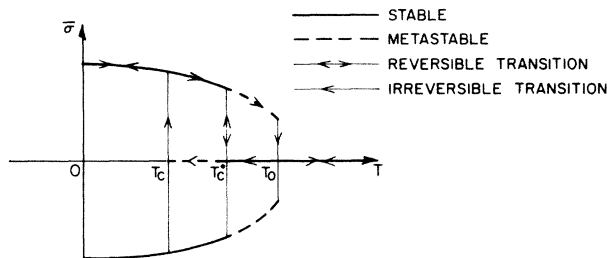


FIG. 5. Plot of the order parameter as a function of temperature for first-order phase transitions.

two different temperature behaviors. If the sample is in a single-domain form (e.g., a monocrystalline solid), then it will stay within a given state until the loss of stability. Therefore, both absolutely stable and metastable situations are admissible and two singular points are expected to manifest themselves at T_c and T_0 . The changes are irreversible and are accompanied by the phenomenon of thermal hysteresis. If, on the other hand, the sample is composed of many domains of local order (e.g., a polycrystalline solid), then a statistically averaged effect will be observed with the actual transition taking place at T_c^* . The change is reversible and T_c^* is the only singular point along the temperature path. The sample is always in the state of absolute stability. In order to distinguish the two types, we will henceforth label the relevant quantities with a prime if they represent the single-domain situation and a double prime if they represent the multiple-domain situation. Figure 6 shows the temperature dependence of the expansion coefficients a_k in both cases and it will have an impact on the corresponding probability distribution and its moments. It is evident that the coefficient a_2 tends to zero as the given phase approaches the end of its stability, i.e., at T_c and T_0 for the disordered and ordered phases, respectively. The probability distribution corresponding to \mathcal{H} of Eq. (36) is

$$P^v(\sigma) = (Z^v)^{-1} \exp\{-v[\mathcal{H}_{LG}(\sigma) + a_2(\sigma - \bar{\sigma})^2 + a_4(\sigma - \bar{\sigma})^4 + a_6(\sigma - \bar{\sigma})^6]\} \quad (38)$$

$$M_n^v = \frac{1}{3} (Z^v)^{-1} \exp[-v\mathcal{H}_{LG}(\bar{\sigma})] (va_6)^{-(n+1)/6}$$

$$\times \left[\sum_{k=0}^{\infty} [-(v/a_6^2)^{1/3} a_4]^k \sum_{m=0}^{\infty} \left[\frac{a_2}{a_4} \right]^m (va_6)^{m/3} \frac{\Gamma((4k-2m+n+1)/6)}{m!(k-m)!} \right]. \quad (39)$$

This is an exact result which is an infinite but convergent series for all T (as long as $V < \infty$). In the lowest order of approximation we have

$$Z^v \cong \frac{1}{3} \exp[-v\mathcal{H}_{LG}(\bar{\sigma})] (va_6)^{-1/6} [\Gamma(\frac{1}{6}) - (va_2)(va_6)^{1/3} \Gamma(\frac{1}{2}) - (va_4)(va_6)^{-2/3} \Gamma(\frac{5}{6}) + \dots] \quad (40)$$

and

$$M_n^v \cong \frac{(va_6)^{-n/6}}{\Gamma(\frac{1}{6})} \left[\Gamma((n+1)/6) + (va_2)(va_6)^{-1/3} \left[\frac{\Gamma((n+1)/6)\Gamma(\frac{1}{2})}{\Gamma(\frac{1}{6})} - \Gamma((n+3)/6) \right] + (va_4)(va_6)^{-2/3} \left[\frac{\Gamma(\frac{5}{6})\Gamma((n+1)/6)}{\Gamma(\frac{1}{6})} - \Gamma((n+5)/6) \right] + \dots \right]. \quad (41)$$

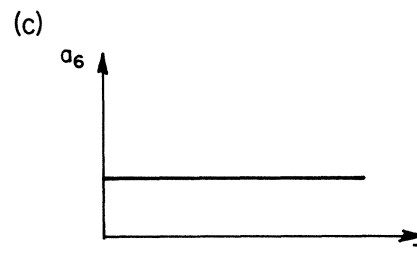
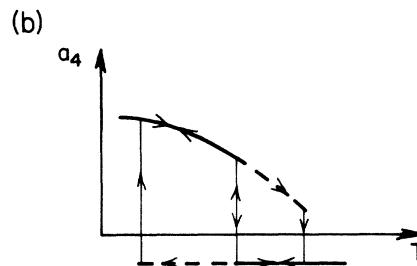
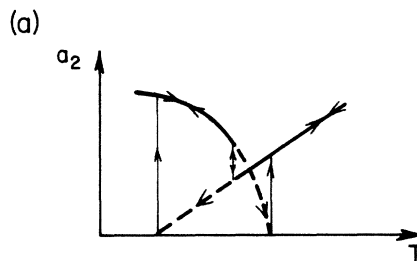


FIG. 6. Plots of the expansion coefficients a_2 (a), a_4 (b), and a_6 (c) for first-order phase transitions. The temperature points are the same as in Fig. 5.

and it is obvious that it is unsuitable for exact calculations. However, given the conclusions of the previous section, we can apply approximate methods of calculation which differ depending on whether $V < \infty$ or $V \rightarrow \infty$. Each of these cases will be treated in turn. In the finite-volume case, the highest-power term must be retained in the exponential and the following series expansion results:

In particular, the susceptibility function has the form

$$\chi^v \cong \frac{v^{2/3} a_6^{-1/3}}{10} \{ 3 - (va_6)^{-1/3} [va_2 + va_4(va_6)^{-1/3}] + \dots \}. \quad (42)$$

As shown in Fig. 7(a), Eq. (42) yields two branches: χ_+^v and χ_-^v which correspond to the two possible phases. These branches tend to zero on either side of T_c^* and attain their finite maxima at T_c and T_0 , respectively. The discontinuity between χ_+^v and χ_-^v at T_c^* , which is measurable in the multiple-domain samples is

$$\Delta\chi^v \equiv (\chi_+^v - \chi_-^v)_{T=T_c^*} \cong 3 \left[\frac{V}{kT_c^*} \right]^{4/3} A_4^2/A_6, \quad (43)$$

and it grows with volume as $V^{4/3}$. As expected at the tricritical point corresponding to $A_4=0$ the discontinuity $\Delta\chi^v$ disappears. The maximum value of susceptibility can then be approximated as

$$\chi_{\max}^v = (\chi_{\pm}^v)_{T=T_c^*} \cong \frac{3}{10} \left[\frac{V}{kT_c^*} \right]^{4/3} a_6^{-1/3}, \quad (44)$$

and it grows in proportionality with $V^{4/3}$. When compared to the corresponding expression for second-order transitions described by sixth-order expansions [see Eq. (42) with $A_4 > 0$ instead of $A_4 < 0$ used before], the susceptibility is less steep around its (comparatively lower) maximum as a result of the change of sign in A_4 and the shift from T_c to T_c^* . It is also interesting to compare Eq. (44) with the corresponding result for the quartic expansion, i.e., Eq. (33) because the two are characterized by entirely different volume scaling, i.e., $V^{4/3}$ and $V^{1/2}$, respec-

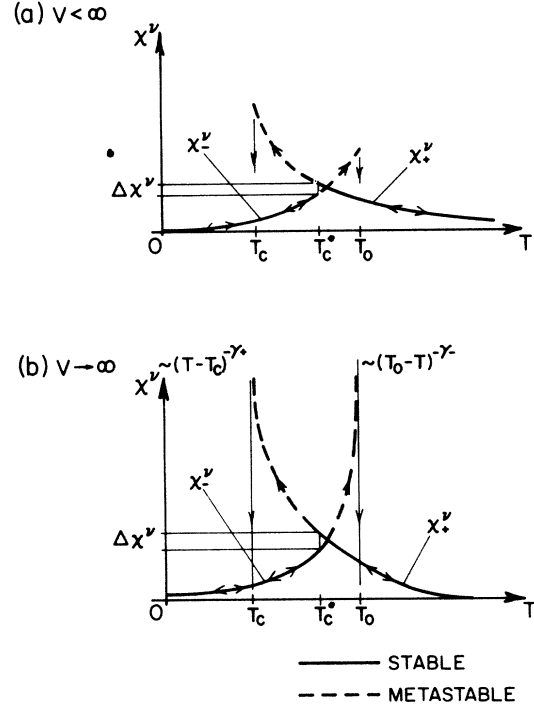


FIG. 7. Plots of χ^v for first-order phase transitions when (a) $V < \infty$ and (b) $V \rightarrow \infty$.

tively.

In the case of the thermodynamic limit, i.e., when $V \rightarrow \infty$, it has been demonstrated in the preceding section that the correct method of calculating M_n^v must retain the lowest-power term in the exponential. The resulting series expansion

$$M_n^v = (Z^v)^{-1} (va_2)^{-(n+1)/2} \exp[-v\mathcal{H}_{LG}(\bar{\sigma})] \left[\sum_{k=0}^{\infty} (-a_6/a_2^3 v^2)^k \sum_{m=0}^k (va_2 a_4/a_6)^m \frac{\Gamma(3k-m+(n+1)/2)}{m!(k-m)!} \right] \quad (45)$$

is convergent (for $V \rightarrow \infty$). On applying the lowest-order volume-scaling corrections, Eq. (45) yields

$$Z^v \cong \exp \left[-v\mathcal{H}_{LG}(\bar{\sigma}) \right] (va_2)^{-1/2} \times \left[\Gamma\left(\frac{1}{2}\right) - \Gamma\left(\frac{7}{2}\right) \frac{a_6}{a_2^3 v^2} - \Gamma\left(\frac{5}{2}\right) \frac{a_4}{a_2^2 v} + \dots \right] \quad (46)$$

and

$$M_n^v \cong (va_2)^{-n/2} \frac{\Gamma((n+1)/2)}{\Gamma\left(\frac{1}{2}\right)} \times \left[1 + \frac{n(n+4)}{4} a_4 (va_2^2)^{-1} + \dots \right]. \quad (47)$$

In particular, the susceptibility function can be approximated by

$$\chi^v \cong (2a_2)^{-1} \left[1 - \frac{6a_4}{va_2} + \dots \right], \quad (48)$$

which is in agreement with the result of the mean-field theory. A plot of χ^v versus T in the thermodynamic limit is shown in Fig. 7(b). The discontinuity in χ^v at $T=T_c^*$ is

$$\Delta\chi^v \cong \frac{3A_6}{2A_4^2} \left[1 - \frac{45A_6}{vA_4} + \dots \right], \quad (49)$$

where the first term is volume independent and the second decreases as V^{-1} . The two branches of χ^v , i.e., χ_+^v and χ_-^v now *diverge* at the two points T_c and T_0 in the single-domain situation. These divergencies signify the loss of stability by the respective metastable phases. We can symbolically write it as

$$\chi_+^v \sim A_+(T-T_c)^{-\gamma_+}, \quad \chi_-^v \sim A_-(T_0-T)^{-\gamma_-}, \quad (50)$$

where A_+, A_- are the critical amplitudes and it is evident

from Eq. (48) that the critical exponents γ_+, γ_- are both 1. The remaining critical exponents will, for both T_0 and T_c , be equal to the mean-field exponents, since the free energy per unit volume is

$$f = \begin{cases} \mathcal{H}_{\text{LG}}(\bar{\sigma}) + \frac{kT}{6V} \ln \left[\frac{a_6 V}{kT} \right] + \dots & \text{for } V < \infty, \\ \mathcal{H}_{\text{LG}}(\bar{\sigma}) + \frac{kT}{2V} \ln \left[\frac{a_2 V}{kT} \right] + \dots & \text{for } V \rightarrow \infty. \end{cases} \quad (51)$$

Once again we emphasize at this point that one of the primary objectives of the present method is to ensure that the uniform convergence criterion is satisfied. This has led to the identification of the two branches of χ^v and to the correct volume scaling by appropriate choice of the expansion coefficients, a_k .

C. Field-induced phase transitions

For field-induced phase transitions⁷ the simplest Landau-Ginzburg Hamiltonian is obtained when \mathcal{H}_{LG} of Eq. (11) is taken with $N=4$ and $A_3=0$. A term describing the interaction with an external field (h) is also added to yield

$$\mathcal{H} = A_2 \sigma^2 + A_4 \sigma^4 - \sigma \cdot h. \quad (52)$$

The equilibrium condition $(\partial \mathcal{H} / \partial \sigma)_{\sigma=\bar{\sigma}}=0$ then results in the equation of state

$$2a(T - T_c)\bar{\sigma} + 4A_4\bar{\sigma}^3 = h, \quad (53)$$

which, in turn, determines the plots of $\bar{\sigma}$ versus h as shown in Fig. 8. Depending on the temperature, there can be two situations. (i) If $T > T_c$, then there is only one

stable phase and $\bar{\sigma} \rightarrow 0$ as $h \rightarrow 0$. (ii) If $T \leq T_c$, then there exist two stable phases in the range $-h_c \leq h \leq h_c$, where

$$h_c = \left(\frac{2}{3}\right)^{3/2} (a |T - T_c|)^{3/2} / (A_4)^{1/2}.$$

However, for a particular h in that range, one of the phases is metastable. As $h \rightarrow 0$, we have $\bar{\sigma} \rightarrow \pm \sigma_0$ where

$$\sigma_0 = (a |T - T_c| / 2A_4)^{1/2}$$

is the amount of spontaneous magnetization. The two possible values of the order parameter can be approximated as follows:

(i) If $|h| \ll h_c$, then

$$\bar{\sigma} \cong \pm \sigma_0 + \chi_0 \cdot h, \quad (54)$$

where

$$\chi_0 = (2a |T - T_c|)^{-1} \text{ for } T > T_c$$

and

$$\chi_0 = (4a |T_c - T|)^{-1} \text{ for } T \leq T_c.$$

(ii) If $|h| \gg h_c$, then

$$\bar{\sigma} \cong (h / 4A_4)^{1/3}. \quad (55)$$

Following the approach adopted in this paper we now expand $\mathcal{H}(\sigma)$ around $\bar{\sigma}$ as

$$\mathcal{H}(\sigma) \cong \mathcal{H}_{\text{LG}}(\bar{\sigma}) + a_2(\sigma - \bar{\sigma})^2 + a_3(\sigma - \bar{\sigma})^3 + a_4(\sigma - \bar{\sigma})^4 + \dots, \quad (56)$$

where $a_2 = A_2 + 6A_4\bar{\sigma}^2 > 0$, $a_3 = 4A_4\bar{\sigma}$, and $a_4 = A_4 > 0$. Obviously, the equilibrium condition precludes the existence of a linear term in Eq. (56). Furthermore, the cubic term may be neglected since it is neither the highest- nor the lowest-power term in the expansion and it only leads to cosmetic corrections. All information pertaining to the field dependence is contained in the expansion coefficients a_k via the expressions for $\bar{\sigma}$ given in Eqs. (54) and (55). We easily find that $a_2 \rightarrow 0$ as $h \rightarrow \pm h_c$ for $T \leq T_c$ and $a_2 > 0$ for all fields h and temperatures $T > T_c$. This is represented in Fig. 9. Note that $A_2 \rightarrow 0$ as $T \rightarrow T_c$. When the cubic term is neglected in the calculations of statistical moments, we can simply use the results of Sec. V A and reinterpret them for the present purposes. Consequently, the n th moment M_n^v is expressed by Eq. (28) and the partition function by Eq. (27). It should, however, be kept in mind that in the present case the variable x is field rather than temperature dependent. Moreover, according to the general classification presented in this section, different plots result for $T \leq T_c$ and $T > T_c$. Within each of the two cases further differences arise depending on whether $V < \infty$ or $V \rightarrow \infty$. The summary of these results is shown in Fig. 10. From the field dependence of a_2 we deduce that for all T the far wings of χ^v are pro-

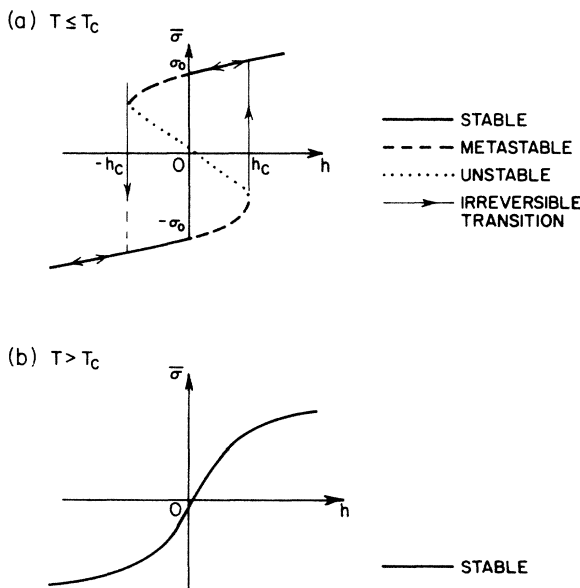


FIG. 8. Plot of the field dependence of the order parameter for (a) $T \leq T_c$ and (b) $T > T_c$.

portional to $|h|^{-2/3}$, while in the thermodynamic limit, the approach to infinity is via $\chi^v \sim |h|^{-2}$. For $T \leq T_c$, there exist two singular points of χ^v corresponding to $\pm h_c$ since the symmetry of the system is broken there. The volume-dependence aspect of the problem is analogous to

that described for second-order temperature-induced phase transitions discussed in Sec. V A.

The following exact results were obtained by expanding the cubic term and integrating with the use of known integrals. The partition function is given by

$$Z^v = \exp[-v\mathcal{H}_{\text{LG}}(\bar{\sigma})] \exp(va_4^2/8a_2)(2va_2)^{-1/4} \sum_{k=0}^{\infty} \frac{\Gamma(3k + \frac{1}{2})}{(2k)!} \left(\frac{\sqrt{v}a_3^2}{2\sqrt{2}(a_2)^{3/2}} \right)^k D_{-3k-1/2} \left[\left(\frac{v}{2a_2} \right)^{1/2} a_4 \right]. \quad (57)$$

Similarly, for even n the n th moment is

$$M_n^v = (Z^v)^{-1} \exp[-v\mathcal{H}_{\text{LG}}(\bar{\sigma})] \exp(va_4^2/8a_2)(2va_2)^{-(n+1)/4} \times \sum_{k=0}^{\infty} \frac{\Gamma(3k + (n+1)/2)}{(2k)!} \left(\frac{\sqrt{v}a_3^2}{2\sqrt{2}(a_2)^{3/2}} \right)^k D_{-3k-(n+1)/2} \left[\left(\frac{v}{2a_2} \right)^{1/2} a_4 \right]. \quad (58)$$

The lowest order of expansions, Eqs. (57) and (58), corresponds to the results of Eqs. (27) and (28). The main effect of including the cubic term is to render the plot of $P^v(\sigma)$ asymmetric with respect to $\bar{\sigma}$, since fluctuations in the direction of the field must be more likely than those against it.

D. Liquid-vapor phase transitions

1. Theory

The essential features of the van der Waals theory of the liquid-vapor critical region can be reproduced using a Landau-type expansion of the phenomenological Hamil-

tonian⁷ in terms of the order parameter $\sigma \equiv \rho - \rho_c$ where ρ is the mean density and ρ_c is its value at the critical point:

$$\mathcal{H} \cong -(p - b\tau)\sigma + A_2\sigma^2 + A_3\sigma^3 + A_4\sigma^4. \quad (59)$$

Here, $\tau \equiv T - T_c$, $A_2 = a\tau$, $a > 0$, and A_3 can be in general of arbitrary sign, but we select $A_3 < 0$ in order for the liquid phase to be stable at low temperatures, $A_4 > 0$ and, finally, $p \equiv P - P_c$ is the reduced pressure. Note that $(p - b\tau)$ plays the role of an external field. Minimization of \mathcal{H} with respect to σ yields an equation of state which

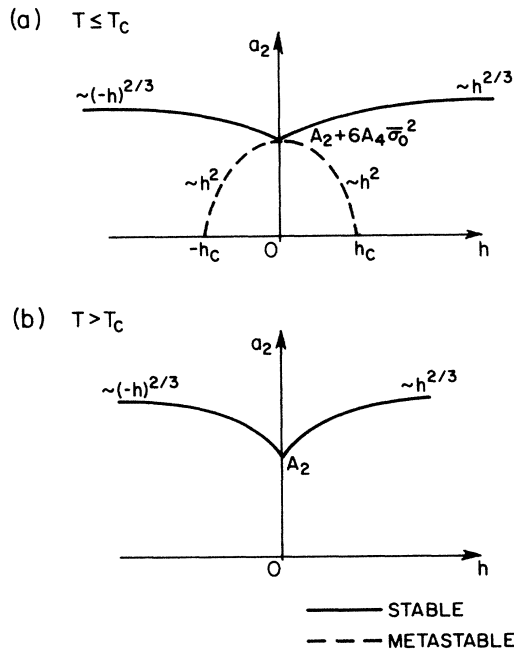


FIG. 9. Plots of the expansion coefficient a_2 for field-induced phase transitions for (a) $T \leq T_c$ and (b) $T > T_c$.

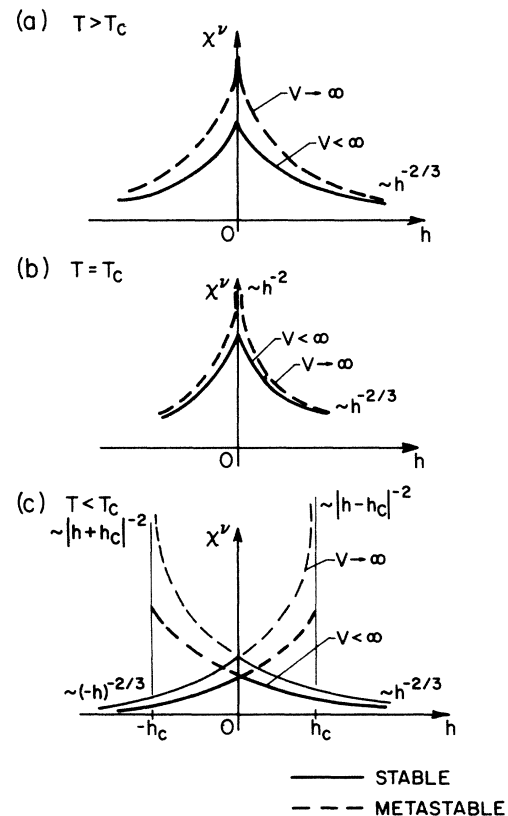


FIG. 10. Plots of χ^v for field-induced phase transitions when (a) $T > T_c$, (b) $T = T_c$, and (c) $T < T_c$.

is equivalent to the van der Waals equation

$$p = b\tau + 2a\tau\sigma + 4A_4\sigma^3, \quad (60)$$

since it leads to the classical critical exponents. The critical isochore corresponds to a straight line $p = b\tau$ on the PT -phase diagram. The critical isotherms are given by $0 = (\partial p / \partial \sigma)_\tau = 2a\tau + 12A_4\sigma^2$, and they also resemble those of the van der Waals theory. The equilibrium phases close to the critical isochore are found to be $\sigma_0 = 0$ and

$$\sigma_\pm = [-3A_3 \pm (9A_3^2 - 32A_2A_4)^{1/2}] / 8A_4.$$

The liquid phase σ_+ is absolutely stable for $T < T_c^* \equiv T_c + A_3^2 / 4aA_4$, the gaseous phase σ_0 is absolutely stable for $T > T_c$, and they coexist in the range $T_c < T < T_c^*$. There is also a gaseous phase corresponding to σ_- which is metastable for $T < T_0$. The actual transition takes place when $\mathcal{H}(\sigma_0) = \mathcal{H}(\sigma_+)$, i.e., at T_c^* . Unless $A_3 = 0$, this is always a first-order phase transition. This transition is illustrated in Fig. 11.

As usual, we can expand $\mathcal{H}(\sigma)$ around $\bar{\sigma}$ according to Eq. (56) with $a_2 = A_2 + 3A_3\bar{\sigma} + 6A_4\bar{\sigma}^2$, $a_3 = A_3 + 4A_4\bar{\sigma}$, and $a_4 = A_4$. The results can be essentially adopted from the preceding section with appropriate reinterpretation. In the present case, the applicable formulas are Eq. (57) for Z^v and Eq. (58) for M_n^v . Their lowest-order approximations are Eqs. (27) and (28), respectively. The plot of χ^v as a function of temperature is shown in Fig. 12. The divergent behavior of χ^v at T_c and T_0 "grows out" of the two branches of χ^v , since $a_2 \rightarrow 0$ as $T \rightarrow T_c$ for χ_-^v and $a_2 \rightarrow 0$ as $T \rightarrow T_0$ for χ_+^v . The volume scaling for each branch of χ^v is the same as that described in Sec. V A for continuous phase transitions. In particular, for $V < \infty$, the approach to the respective maxima is via an exponential function as shown in Eqs. (29) and (30). The difference is, of course, that now each of two metastable phases has an associated divergence in the thermodynamic limit. In fact, it may be of some significance to note that within the framework presented here one can classify second-order phase transitions as a limiting case of first-order phase transitions, when the two singular points (associated with the first-order case) coincide.

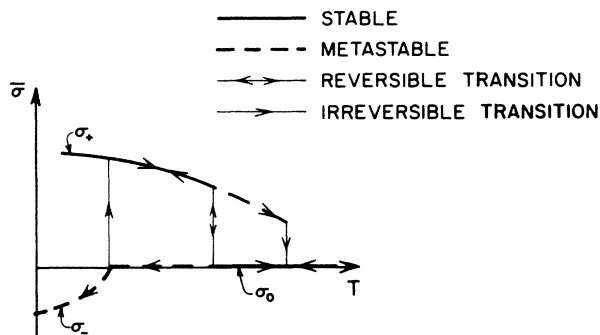


FIG. 11. Plot of the temperature dependence of the order parameter for liquid-vapor phase transitions.

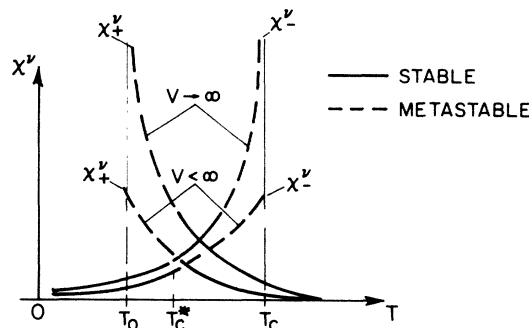


FIG. 12. Plot of χ^v for liquid-vapor phase transitions.

2. Experiment

The experimental investigation of inhomogeneities in the density of near-critical fluids has played an important role in the development of current theories of the critical phenomenon. In particular, the techniques of elastic photon-neutron scattering have yielded information pertaining to the size and lifetime of these density fluctuations. However, information regarding the probability of occurrence $P(\rho)$ of different local densities (ρ) has not been accessible to experiment and has not played a significant role in theoretical developments.

It is therefore of importance that recent experiments^{5,6} have demonstrated the effectiveness of vibrational Raman scattering as a probe of the $P(\rho)$ distribution near the liquid-vapor critical point in molecular nitrogen. The technique relies upon the sensitivity of the vibrational motion in a given molecule to the field created by its neighbors. This field has a range of about 1 nm, as determined by the pair potential, and defines a local density ρ within a probed volume whose dimensions are orders of magnitude smaller than the correlation lengths normally expected near the critical point (see Fig. 13). Given a substantial background of experiment and theory for the normal fluid, it is determined^{5,6} that as the critical point is approached the slow, large-amplitude fluctuations in ρ give rise to an inhomogeneous broadening which dominates the spectrum in particular cases (e.g., N_2, H_2). This phenomenon is somewhat analogous to Doppler broadening in a low-density gas, with the difference that the statistical variable is ρ rather than the molecular velocity.

The resulting experimental information, which was obtained along the critical isochore, is summarized in Fig. 14. It demonstrates that the second moment of $P(\rho)$, which is here designated as M_2 , varies exponentially with ϵ as it approaches a maximum value at the critical point. This behavior is in agreement with that predicted by Eq. (28) with $n = 2$, or its depiction in Fig. 4, but it must be emphasized that the comparison is limited to the range $\epsilon \leq 10^{-2}$ where the experiment is most sensitive. Except for details which are beyond the scope of both the experiment^{5,6} and the mean-field theory, there is also substantial agreement with recent Monte Carlo simulations¹⁷ of finite-size effects in near-critical magnetic systems. More specifically, the proportionality of χ_{\max}^v to the square root

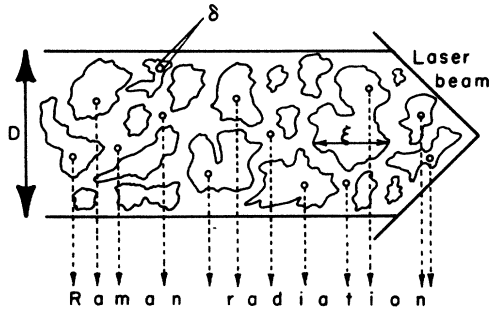


FIG. 13. Schematic representation of the Raman scattering experiment described in Refs. 5 and 6. The laser beam with $D \sim 10\text{--}100 \mu\text{m}$ illuminates a small volume within a much larger ($\sim 1 \text{ cm}^3$) bulk sample which is maintained under conditions very near the liquid-vapor critical point. Each Raman event probes the density in a spherical volume whose diameter ($\delta \sim 1 \text{ nm}$) is much smaller than the correlation lengths ξ ($\sim 1 \mu\text{m}$) normally expected. The Raman signal is integrated over time.

of the sample's volume as shown in Eq. (33) is in agreement with the computer simulation result. Certain features, however, are absent in our model. The plot of χ^v has a cusplike shape and the critical temperature does not shift with volume. These characteristics are undoubtedly drawbacks of our simple model and they are most likely caused by the absence of dynamical correlations. This latter aspect is currently under investigation by the authors and we hope to be able to include it in a future publication treating dynamical correlations in a non-Gaussian manner.

VI. SUMMARY AND CONCLUSION

The well-known theoretical model employed in this paper was originated by Landau and Ginzburg.⁷ We have adopted the position that the Gaussian approximation which is usually employed with the Landau-Ginzburg model is an unnecessary approximation which leads to significant restrictions upon the applicability of the model, especially in the regime of large fluctuations. The predictions of the model have therefore been examined for a particular class of non-Gaussian distributions which is obtained as a generalization of the Gaussian and which includes it as a special case. Emphasis is placed upon the rigor of the mathematics and, in particular, upon strict adherence to the uniform convergence criterion. In view of the results obtained, the treatment is justified in two ways: (i) The non-Gaussian distributions lead to results for finite-sample volumes which are qualitatively different from Gaussian predictions and also more plausible, because the unphysical divergences which are associated with the Gaussian approximation are eliminated. (ii) For the particular case of the liquid-vapor transition, the predicted behavior of $P(\rho)$ is in qualitative agreement with recent experimental results.^{5,6} Generally speaking, the predictions of the mean-field theory are also consistent with the Monte-Carlo simulations of Binder¹⁷ for

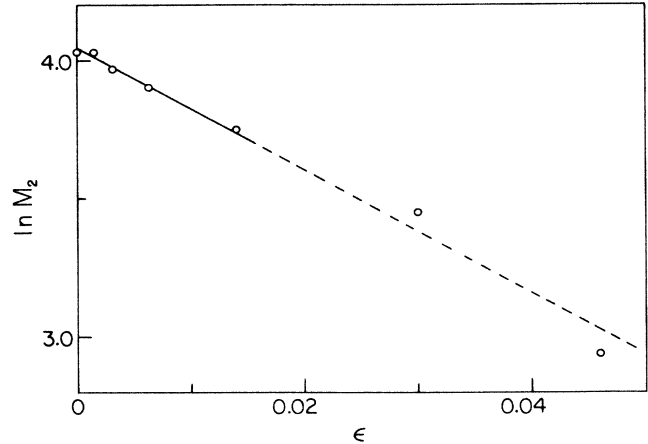


FIG. 14. Natural logarithm of the square root of the $P(\rho)$ second moment, M_2 (in units of ρ/ρ_{stp}) versus ϵ on the critical isochore of fluid N_2 . The diagram is reproduced from Ref. 6. The linear fit corresponds to $M_2 = 60\exp(-23\epsilon)$ and the dashed extension indicates the region where the determination of M_2 is not considered reliable.

finite magnetic systems in the near-critical regime. The finer details displayed by these (Monte Carlo) results are beyond the scope of the mean-field approach and pose a challenge for future work.

Our basic conclusion is, therefore, that removal of the Gaussian restriction leads to further significant contributions from the Landau-Ginzburg model. It is apparent that the introduction of the quartic (i.e., first) non-Gaussian term is the most important step in the generalization process, because higher-order terms do not give rise to any further significant differences in the qualitative behavior. As suggested in the context of the renormalization-group approach,^{2,3} the primary effect of the quartic term seems to be that it more satisfactorily simulates the physical bounds which are imposed on σ . In liquid-vapor systems, for example, there is the strict requirement that $\rho \geq 0$ (i.e., $\sigma_{\min} = -\rho_c$), while the values of ρ greater than the triple point value must be regarded as extremely improbable [i.e., $\sigma_{\max} \cong (\rho_{tp} - \rho_c)$]. Clearly then the correct expression for the partition function is

$$Z = \int_{\sigma_{\min}}^{\sigma_{\max}} e^{-\beta\mathcal{H}(\sigma)} d\sigma.$$

The assumption implicit in the present treatment [see Eq. (21), for example] is that the radius of convergence of such an integral lies entirely within the bounds of the physically admissible values of σ , so that infinite limits of integration can be used for mathematical convenience. While this assumption is consistent with the experimental result of Refs. 5 and 6, there is no reason to expect that it is always valid. If, for example, $P(0)$ were not negligible, then $P(\rho)$ distribution would be discontinuous at $\rho=0$ and an alternative approach would be required.

ACKNOWLEDGMENTS

The authors wish to thank Professor K. Binder for helpful comments and for access to unpublished Monte

Carlo results. This research has been supported by grants from the Natural Sciences and Engineering Research Council of Canada.

APPENDIX A

The statistical moments M_n of the Gaussian distribution are calculated using the following Gaussian integral¹⁸:

$$\int_0^{\infty} x^{\nu-1} e^{-\mu x^p} dx = \begin{cases} \frac{1}{|p|} \mu^{-\nu/p} \Gamma(\nu/p) & \text{if } \mu > 0 \\ \infty & \text{if } \mu \leq 0 \end{cases} \quad (\text{A1})$$

as

$$M_n \equiv \frac{1}{\sqrt{2\pi\lambda}} \int_{-\infty}^{+\infty} x^n \exp\left[-\frac{x^2}{2\lambda_2}\right] dx = \begin{cases} \frac{1}{\sqrt{\pi}} \Gamma((n+1)/2) (2\lambda_2)^{n/2} \\ 0 & \text{if } n \text{ is odd.} \end{cases} \quad (\text{A2})$$

APPENDIX B

The partition function Z and the n th moment M_n corresponding to the series expansion of the probability distribution function of Eq. (17) are calculated using Eq. (A1) as $Z = I_0$ and $M_n = I_n/I_0$, where

$$I_n \equiv \int_{-\infty}^{+\infty} x^n \exp(-\lambda_2 x^2 - \lambda_4 x^4) dx = 2 \sum_{k=0}^{\infty} \frac{1}{k!} \int_0^{\infty} (-\lambda_4)^k x^{4k+n} \exp(-\lambda_2 x^2) dx = (\lambda_2)^{-(n+1)/2} \sum_{k=0}^{\infty} \left[\frac{\lambda_4}{\lambda_2^2} \right]^k \frac{\Gamma((4k+n+1)/2)}{\Gamma(k)} \quad (\text{B1})$$

if n is even and $I_n = 0$ if n is odd. A simple quotient test applied to I_n with the aid of the formula¹⁵

$$\frac{\Gamma(z+a)}{\Gamma(z+b)} \rightarrow z^{a-b} [1 + O(1/z)] \text{ as } z \rightarrow \infty \quad (\text{B2})$$

gives

$$\lim_{k \rightarrow \infty} \frac{a_{k+1}}{a_k} = \left[-4 \frac{\lambda_4}{\lambda_2^2} \right] \lim_{k \rightarrow \infty} k,$$

which indicates that I_n is divergent except when $\lambda_4 = 0$ or $\lambda_2 = +\infty$. For $M_n \equiv I_n/I_0$ we obtain in the asymptotic limit, since it is a ratio of two divergent series,

$$M_n \sim (\lambda_2)^{-n/2} \lim_{k \rightarrow \infty} (2k)^{n/2} \quad (\text{B3})$$

which diverges unless $\lambda_2 \rightarrow \infty$.

APPENDIX C

The partition function Z and the n th moment M_n corresponding to the series expansion of the probability distribution function of Eq. (20) are calculated using Eq. (A1) and

$$I_n = 2 \sum_{k=0}^{\infty} \frac{1}{k!} \int_0^{\infty} (-\lambda_2)^k x^{2k+n} \exp(-\lambda_4 x^4) dx = \frac{1}{2} (\lambda_4)^{-(n+1)/4} \sum_{k=0}^{\infty} \left[-\frac{\lambda_2}{(\lambda_4)^{1/2}} \right]^k \frac{\Gamma((2k+n+1)/4)}{\Gamma(k)}. \quad (\text{C1})$$

A simple quotient test performed for I_n using Eq. (B2) yields

$$\lim_{k \rightarrow \infty} \frac{a_{k+1}}{a_k} = \left[-\frac{\lambda_2}{(2\lambda_4)^{1/2}} \right] \lim_{k \rightarrow \infty} \frac{1}{\sqrt{k}},$$

which is convergent unless $\lambda_2 \rightarrow \infty$ or $\lambda_4 = 0$. Consequently, both Z and M_n are finite for all values of λ_2 and λ_4 except $\lambda_4 = 0$ and $\lambda_2 = \infty$, i.e., when $\lambda_2/(\lambda_4)^{1/2} \rightarrow \infty$.

APPENDIX D

Recently, Witschel¹⁴ published a very useful integral

$$\int_0^{\infty} x^{2k\nu-1} \exp(-ax^{4k} - bx^{2k}) dx = (2k)^{-1} (2a)^{-\nu/2} \Gamma(\nu) \exp(b^2/8a) D_{-\nu}(b/(2a)^{1/2}), \quad (\text{D1})$$

where $D_{-\nu}$ is the parabolic cylinder function.¹⁵ In our case we simply substitute $k=1$, $\nu=(n+1)/2$, $a=\lambda_4$, $b=\lambda_2$, and obtain compact analytical expressions for Z and M_n

$$Z = (2\lambda_4)^{-1/4} \Gamma\left(\frac{1}{2}\right) \exp\left[\frac{\lambda_2^2}{8\lambda_4}\right] D_{-1/2}(\lambda_2/(2\lambda_4)^{1/2}) \quad (\text{D2})$$

and

$$M_n = (2\lambda_4)^{-n/2} \frac{\Gamma((n+1)/2)}{\Gamma\left(\frac{1}{2}\right)} \frac{D_{-(n+1)/2}(\lambda_2/(2\lambda_4)^{1/2})}{D_{-1/2}(\lambda_2/(2\lambda_4)^{1/2})}. \quad (\text{D3})$$

APPENDIX E

In the general case of the probability distribution function given by Eq. (25), and assuming both p and q even, we find by its series expansion that

$$I_n = \sum_{k=0}^{\infty} \frac{1}{k!} \int_{-\infty}^{+\infty} x^n (-\lambda_p x^p)^k \exp(-\lambda_q x^q) dx = \sum_{k=0}^{\infty} \frac{(\lambda_q)^{-(n+1)/q}}{q} \frac{1}{k!} \left[-\frac{\lambda_p}{\lambda_q^{p/q}} \right]^k \Gamma((n+pk+1)/q). \quad (\text{E1})$$

Then, the quotient test yields for Z

$$\lim_{k \rightarrow \infty} \frac{a_{k+1}}{a_k} = \left[-\frac{\lambda_p}{\lambda_q^{p/q}} \right] \left[\frac{p}{q} \right]^{p/q} \lim_{k \rightarrow \infty} k^{p/q-1}.$$

Therefore, we conclude that the series expansion with $p > q$ is convergent whenever $\lambda_p = 0$ or $\lambda_q \rightarrow \infty$, or $\lambda_p/\lambda_q^{p/q} \rightarrow 0$; the one with $p < q$ converges whenever $\lambda_p \neq 0$ and $\lambda_q < \infty$. It can similarly be demonstrated that the same criterion applies to $M_n = I_n/I_0$. In our physical applications we will be dealing with both cases in various situations.

- ¹S.-k. Ma, *Modern Theory of Critical Phenomena* (Benjamin, Reading, Mass., 1976).
- ²M. E. Fisher, in *Renormalization Group in Critical Phenomena*, edited by J. D. Gunton and M. S. Green (Temple University Press, Memphis, 1974).
- ³M. E. Fisher, in *Critical Phenomena, Lecture Notes in Physics* (Springer-Verlag, Berlin, 1983).
- ⁴J. A. Tuszyński, M. J. Clouter, and H. Kiefte, *Phys. Lett.* **108A**, 272 (1985).
- ⁵M. J. Clouter and H. Kiefte, *Phys. Rev. Lett.* **52**, 763 (1984).
- ⁶M. J. Clouter, H. Kiefte, and C. G. Deacon, *Phys. Rev. A* (to be published).
- ⁷L. D. Landau and E. M. Lifshitz, *Statistical Physics* (Pergamon, London, 1959).
- ⁸M. Toda, R. Kubo, and N. Saito, *Statistical Physics I* (Springer-Verlag, Berlin, 1983).
- ⁹H. E. Stanley, *Introduction to Phase Transitions and Critical Phenomena* (Oxford University Press, New York, 1971).
- ¹⁰C. N. Yang and T. D. Lee, *Phys. Rev.* **87**, 404 (1952).
- ¹¹J. S. Rowlinson, *Liquids and Liquid Mixtures* (Butterworth, London, 1969).
- ¹²(a) V. Privman and M. E. Fisher, *J. Stat. Phys.* **33**, 385 (1983); (b) *Phys. Rev. B* **30**, 322 (1984); (c) V. Privman, *Physica A* **123**, 428 (1984); (d) H. J. Hermann and D. Stauffer, *Phys. Lett. A* **100**, 366 (1984); (e) K. Binder, *Z. Phys. B* **43**, 119 (1981); (f) A. D. Bruce, *J. Phys. C*, **14**, 3667 (1981).
- ¹³D. J. Wallace, in *Solitons and Condensed Matter Physics*, edited by A. R. Bishop and T. Schneider (Springer-Verlag, Berlin, 1981).
- ¹⁴(a) W. Witschel, *Chem. Phys.* **50**, 265 (1980); (b) *Z. Naturforsch.* **36A**, 481 (1981).
- ¹⁵*Handbook of Mathematical Functions*, edited by M. Abramowitz and I. A. Stegun (Dover, New York, 1965).
- ¹⁶G. Arfken, *Mathematical Methods for Physicists* (Academic, Orlando, 1985).
- ¹⁷(a) K. Binder (private communication); (b) K. Binder, *Critical Properties and Finite-Size Effects of the Five-Dimensional Ising Model*, *Z. Phys.* (to be published); (c) K. Binder, M. Nauenberg, V. Privman, and A. P. Young, *Phys. Rev. B* **31**, 1498 (1985).
- ¹⁸I. S. Gradshteyn and I. M. Ryzhik, *Table of Integrals, Series and Products* (Academic, New York, 1965).